

New homoleptic bis(pyrrolylpyridylimino) Mg(II) and Zn(II) complexes as catalysts for the ring opening polymerization of cyclic esters *via* an "activated monomer" mechanism.



UNIVERSITÀ DEGLI STUDI DI SALERNO
Dipartimento di Chimica e Biologia
"Adolfo Zambelli"



Editorial Office, Dalton Transaction
Cambridge

Fisciano, 5th July 2017

Dear Editor,

attached please find a manuscript entitled: *homoleptic bis(pyrrolylpyridiylimino) Mg(II) and Zn(II) complexes as catalysts for the ring opening polymerization of cyclic esters via an "activated monomer" mechanism.* by Ilaria D'Auria, Consiglia Tedesco, Mina Mazzeo and myself, that we are submitting for publication in *Dalton Transaction* as a *Full Paper*.

In this manuscript, we report the synthesis of new homoleptic bis(pyrrolylpyridiylimino) magnesium and zinc complexes, their structural characterization both in solution and in the solid state, and their application as catalysts for the ring opening polymerization (ROP) of cyclic esters. Noteworthy, the magnesium complex showed high activity in the ROP of ϵ -caprolactone and an extremely high activity in the ROP of lactide under mild conditions. A detailed NMR study revealed that the polymerization proceeds via an *activated monomer* mechanism, involving the coordinative flexibility of the ligands. These findings indicate that this approach can be a potent method to produce polyesters in a controlled way and suggest alternative routes to catalyst design.

On the basis of the above results and considering the broad interest for the synthesis of aliphatic polyesters in both the academic and the industrial scientific communities, we believe that this study is worthy of publication in *Dalton Transactions*:

I hereby state that this manuscript has not been published elsewhere and is not under consideration for publication anywhere in any medium whatsoever.

Sincerely,

Claudio Pellecchia

Professor of Inorganic Chemistry

New homoleptic bis(pyrrrolylpyridiylimino) Mg(II) and Zn(II) complexes as catalysts for the ring opening polymerization of cyclic esters via an "activated monomer" mechanism.

Ilaria D'Auria,^{1,2} Consiglia Tedesco,¹ Mina Mazzeo^{1,2} and Claudio Pellecchia^{1,2*}

Abstract

The reaction of MgBu_2 and ZnEt_2 or $\text{Zn}[\text{N}[\text{Si}(\text{CH}_3)_2]_2]$ with a tridentate monoanionic pyrrolylpyridiylimino $[\text{N},\text{N},\text{N}]$ proligand gave the homoleptic species, as exclusive products, in high yields. The complexes were characterized in solution by 1D and 2D NMR analysis and by single crystal X-ray crystallography. The new homoleptic complexes were tested as initiators in the polymerization of ϵ -caprolactone and lactide in the presence of an exogenous alcohol. For both complexes, the polymerizations proceed via an "activated monomer" mechanism that, in the case of the magnesium complex, was correlated with the coordinative flexibility of the ligands, resulting in extremely high productivities under mild conditions.

Introduction

Aliphatic polyesters have recently gained considerable attention as an environmentally friendly class of polymeric materials.¹ The most promising members of this class are poly(lactide) (PLA) and polycaprolactone (PCL). PLA in particular, because of its favorable mechanical properties and the fact that it can be produced from inexpensive renewable resources, has been applied in numerous fields such as green packaging and fiber technology. Moreover, as biocompatible materials, PLA and PCL have a consolidated role in the field of biomedical applications.²

Among the different synthetic methods suitable for production of polyesters, the ring-opening polymerization (ROP) of the related cyclic esters promoted by metal complexes is, unequivocally, the most effective route to obtain polymers with controlled microstructure and narrow distributions of molecular weights.

In the last years, a plethora of metal catalysts has been described for ROP of cyclic esters.^{3,4} Among these, the complexes based on biologically benign metals complexes have a special role,⁵⁻⁹ since for the production of materials for biomedical applications the complete removing of the catalyst

residues requires high efforts.

Interesting examples of "single-site" initiators for ROP of cyclic esters are complexes of divalent metals of the type LM-X, formed by zinc^{10,11} and magnesium centres supported by β -diketiminato,¹²⁻¹⁵ trispyrazolylborate¹⁶, N-heterocyclic carbene^{17,18} or phenolate based ligands.¹⁹⁻²⁷ Although homoleptic metal complexes are not traditionally qualified as potentially effective initiators for ROP of cyclic esters, recent studies showed that homoleptic compounds of type ML_2 , in combination with an exogenous alcohol, can be very promising catalytic systems.^{28,29}

Recently, we introduced a new family of tridentate dianionic $[\text{N},\text{N},\text{N}]$ pyrrolylpyridiylamido-based ligands into the chemistry of group 3³⁰ and Group 4³¹⁻³⁴ metals. In this contribution we have extended the scope of this ligand framework, designing a monoanionic pyrrolylpyridiylimino ligand $[\text{N},\text{N},\text{N}]$ to explore the coordination chemistry of bivalent metals.

Herein we report the synthesis and structural characterization of magnesium and zinc complexes supported by such $[\text{N},\text{N},\text{N}]$ ligand and their application as initiators for cyclic esters polymerization.

Results and discussion

Synthesis and NMR characterization of the pyrrolylpyridiylimino complexes

The pyrrolylpyridiylimino pro-ligand 6-(1H-Pyrrol-2-yl)-2-(2,6-diisopropylphenyl)iminopyridine (NNN-H) was synthesized following previously reported procedures.^{35,36} We initially

¹Dipartimento di Chimica e Biologia "A. Zambelli", Università di Salerno, via Giovanni Paolo II 132 - 84084 Fisciano (SA) Italy.

²Consorzio Interuniversitario Reattività Chimica e Catalisi (CIRCC), via Celso Ulpiani 27 - 70126 Bari (Italy)

Electronic Supplementary Information (ESI) available: CCDC 1554856-1554857 contain the supplementary crystallographic data for this paper. For ESI and crystallographic data in CIF format see DOI: 10.1039/x0xx00000x

targeted the synthesis of heteroleptic (NNN)Mg-(*n*-Bu), *via* alkane elimination reaction between the monoanionic tridentate pro-ligand NNN-H and one equiv of Mg(*n*-Bu)₂. However, the reaction performed at 25 °C in dry benzene afforded the homoleptic species [NNN]₂Mg (**1**), a deep orange solid, as the only product. Attempts to prepare the heteroleptic complex by changing reaction parameters (e.g. temperature, concentration, solvent, slow addition of reagents) failed.

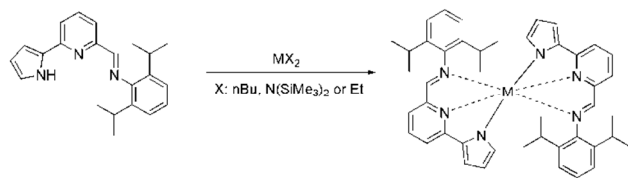
Similarly, the reaction of the pro-ligand NNN-H with Zn{N[Si(CH₃)₃]₂}₂ or Zn(C₂H₅)₂ led invariably, under a variety of reaction conditions, to the isolation of the homoleptic complex [NNN]₂Zn (**2**), as a red solid (Scheme 1). Complexes **1** and **2** were fully characterized by multinuclear NMR spectroscopy and elemental analyses.

The ¹H NMR spectrum of complex **1** showed no high field signals attributable to the *n*-butyl protons bound to the metal centre, as expected for the homoleptic bis chelate complex. A single set of resonances for the two symmetrically coordinated ligands, the disappearance of the resonance of the N-H groups and the concomitant appearance of two different resonances for the diastereotopic methyl protons of the isopropyl groups confirmed the proposed structure (see Figure 1).

For complex **1**, full resonance assignment (see Figure 1) was obtained by following the scalar and/or dipolar connectivity in 1D and 2D homo- and hetero-nuclear NMR experiments (¹H COSY, ¹H NOESY and ¹³C{¹H} HMBC).

The H10 resonance (δH = 8.08 ppm, see Figure 1 for numbering), easily recognized since it is the only singlet integrating for one proton in the ¹H NMR spectrum, was considered as the starting point.

NOE experiments allowed to discriminate between protons H8 and H6 because of the NOE interaction of proton H8 with imine proton H10. Similarly, H3 was discriminated from H1 because of the NOE contact with proton H6 (see Figure 2 B).



Scheme 1. Synthesis of complexes **1** (M = Mg) and **2** (M = Zn)

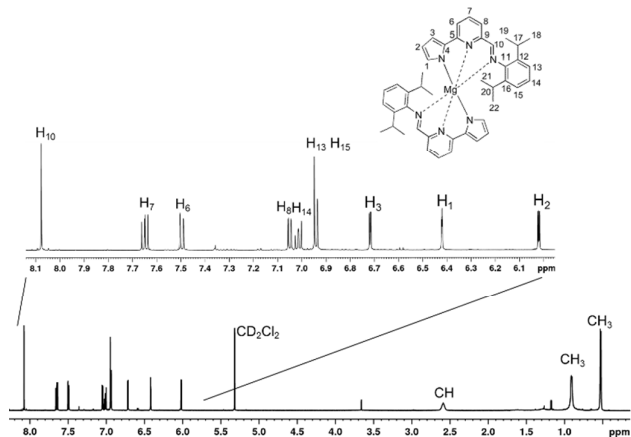


Figure 1. ¹H NMR spectrum (CD₂Cl₂, 298 K, 600 MHz) of magnesium complex **1**.

The patterns of NOE contacts between three protons of the pyrroly moiety (H1', H2' and H3') and the methyl of isopropyl (H19 and H21) suggest that two ligand moieties are coordinated around the metal central in an approximately perpendicular arrangement, in which a pyrrolyl group of one ligand interacts with the isopropyl groups of the other ligand.

The NOE contact between the methyl protons H19 and H21 of the isopropyl groups and the proton H8 of the pyridine moieties suggests a slow rotation of the isopropyl groups around the C12-C17 and C16-C20 single bonds.

NMR spectral assignments for the zinc complex **2** have been obtained by following the same line of reasoning as for **1**. The corresponding proton and carbon chemical shift values are reported in the supporting information. The NMR analyses of the zinc complex **2** resulted in structural features similar to those discussed for complex **1**. In the ¹H-NMR spectrum of **2**, however, the methyl and methine signals of the isopropyl groups were much sharper, suggesting a higher fluxionality of the imine fragments derived from a fast rotation of the isopropyl groups around the C12-C17 and C16-C20 single bonds (see Figure 4).

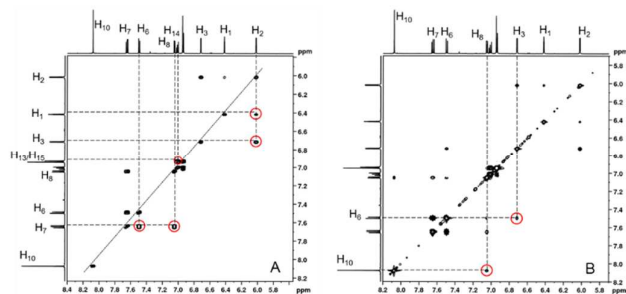


Figure 2. A: a section of the ¹H COSY NMR spectrum of **1** (600 MHz, CD₂Cl₂, 298 K) and B: a section of NOESY NMR spectrum of **1** (600 MHz, CD₂Cl₂, 298 K).

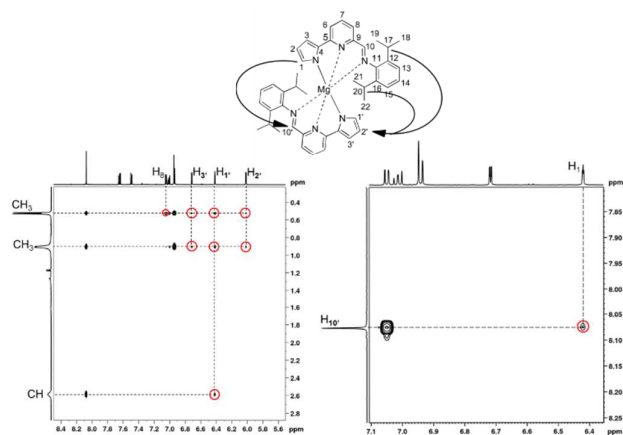


Figure 3. Two sections of the ^1H NOESY NMR spectrum of **1** (600 MHz, CD_2Cl_2 , 298 K).

Additionally, the NOE contacts between the H1 and H10' protons of the coordinated ligands and between the protons of pyrrolyl moiety and the methyl of isopropyl groups were not detected (see figure S6B). The origin of these differences has been clarified by the X-ray diffraction studies of **1** and **2** (*infra*).

X-ray structural analysis

The solid state molecular structures of complexes **1** and **2** were established by single-crystal X-ray diffraction studies. X-ray diffraction quality single crystals of both compounds were obtained as toluene solvates by crystallization from toluene solutions at -20°C . The X-ray molecular structures are shown in Figures 5 and 6, respectively. Selected bond distances and angles are listed in Table 1.

The magnesium atom in compound **1** is six-coordinate, adopting a distorted octahedral geometry with two tridentate ligands almost perpendicular to each other, the dihedral angle between the ligand mean planes being $78.05(3)^\circ$.³⁷ Each ligand assumes an almost planar geometry within a rmsd of 0.055 \AA and 0.077 \AA , with the isopropyl substituted aromatic moieties tilted by $65.77(4)^\circ$ and $54.92(6)^\circ$, respectively.

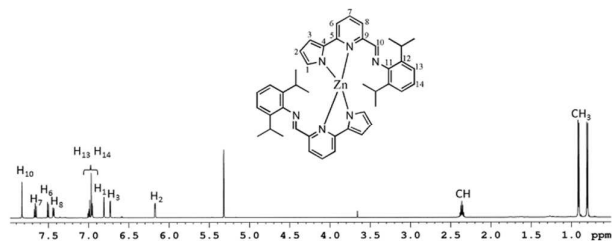


Figure 4. ^1H NMR spectrum (CD_2Cl_2 , 298 K, 600 MHz) of zinc complex **2**.

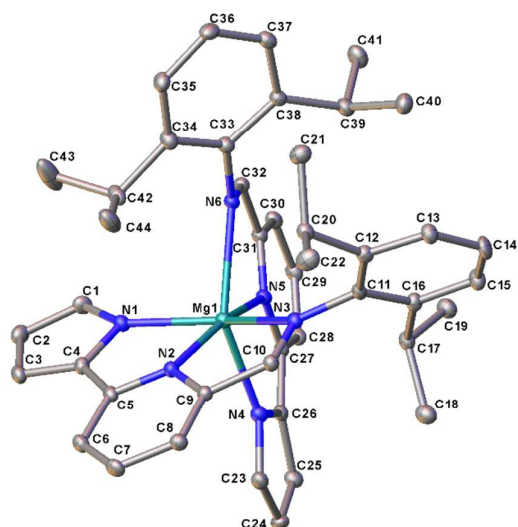


Figure 5. ORTEP drawing of compound **1**. Hydrogen atoms have been omitted for clarity. Ellipsoids are drawn at 20% probability level.

Pyridine nitrogen atoms N2 and N5 feature the shortest distances with the magnesium atom, $2.108(3) \text{ \AA}$ and $2.125(3) \text{ \AA}$, respectively; pyrrolyl nitrogen atoms N1 and N4 are at intermediate distances, $2.145(3) \text{ \AA}$ and $2.137(3) \text{ \AA}$, respectively, while imine nitrogen atoms N3 and N6 feature the longest bond distances with the metal atom, $2.436(3) \text{ \AA}$ and $2.382(3) \text{ \AA}$, respectively.

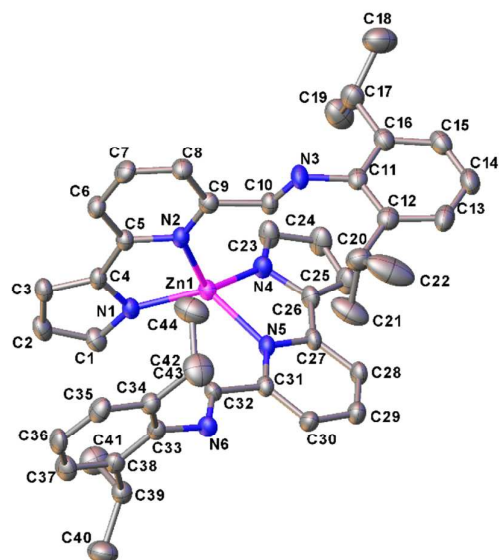


Figure 6. ORTEP drawing of compound **2**. Hydrogen atoms have been omitted for clarity. Ellipsoids are drawn at 20% probability level.

Table 1. Selected bond lengths (Å) and angles (°) for compounds **1** and **2**.

1		2	
Mg1—N1	2.145(3)	Zn1—N1	1.921(5)
Mg1—N2	2.108(3)	Zn1—N2	2.086(5)
Mg1—N3	2.436(3)	Zn1—N4	1.932(5)
Mg1—N4	2.137(3)	Zn1—N5	2.086(5)
Mg1—N5	2.125(3)		
Mg1—N6	2.382(3)		
N1—Mg1—N2	76.86(11)	N5—Zn1—N2	113.82(19)
N1—Mg1—N3	145.37(11)	N1—Zn1—N2	84.3(2)
N1—Mg1—N4	99.99(11)	N1—Zn1—N5	122.5(2)
N1—Mg1—N5	93.44(11)	N1—Zn1—N4	134.6(2)
N1—Mg1—N6	93.91(10)	N4—Zn1—N2	120.3(2)
N2—Mg1—N3	71.80(10)	N4—Zn1—N5	84.2(2)
N2—Mg1—N4	90.80(11)		
N2—Mg1—N5	162.12(11)		
N2—Mg1—N6	123.02(11)		
N3—Mg1—N4	94.88(10)		
N3—Mg1—N5	120.57(10)		
N4—Mg1—N5	75.95(11)		
N4—Mg1—N6	145.69(11)		
N5—Mg1—N6	72.01(10)		

The zinc atom in compound **2** is four-coordinate with a distorted tetrahedral geometry, with two bidentate ligands perpendicular to each other, the dihedral angle between the ligand mean planes being 89.57(9)°.³⁷

Each ligand assumes an almost planar geometry within a rmsd of 0.030 Å and 0.052 Å, with the isopropyl substituted aromatic moieties tilted by 84.56(14)° and 84.92(14)°, respectively.

Pyrrolyl nitrogen atoms N1 and N4 feature the shortest distances with the zinc atom, 1.921(5) Å and 1.932(5) Å, respectively, while pyridine nitrogen atoms N2 and N5 feature the longest distances with the zinc atom, being both 2.086(5) Å. Imine nitrogen atoms N3 and N6 are not coordinated to Zn and display both an anti relationship with nitrogen atoms N2 and N5 respectively.

The different coordination geometries observed in the solid state molecular structures for the two complexes are retained in solution, as emerged by the discussion of the NMR spectra (see above).

Ring opening polymerization of ϵ -caprolactone

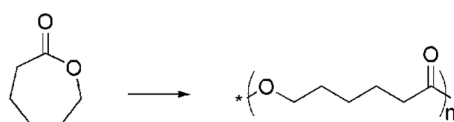
Complexes **1** and **2** were evaluated as catalysts in the ring-opening polymerization (ROP) of ϵ -caprolactone (ϵ -CL). Polymerization screenings were performed under a nitrogen atmosphere in toluene solution of ϵ -CL and the proper metal compound (scheme 2).

The obtained polymers were characterized by ¹H NMR and GPC analyses. Representative results are collected in Table 2.

Complex **1** resulted an efficient initiator for the polymerization of ϵ -CL producing high molecular weight polymers. At room temperature, complex **1** was able to convert about 150 equiv. of monomer in 100 minutes (run 1, Table 2).

The obtained polymer showed a monomodal and narrow molecular weight distribution (Mw/Mn = 1.09) although the experimental (corrected) number-average molecular weights were several times larger than the calculated values. This suggested that only a fraction of magnesium complex was involved in catalysis.

Increasing the temperature to 100 °C led to substantial raise of the activity (200 equivalents of monomer were converted within 5 min), but with an increase in the polydispersity index (Table 2, run 1 vs run 2), possibly as a consequence of intramolecular transesterification processes.



Scheme 2. Polymerization of ϵ -caprolactone promoted by **1** and **2**

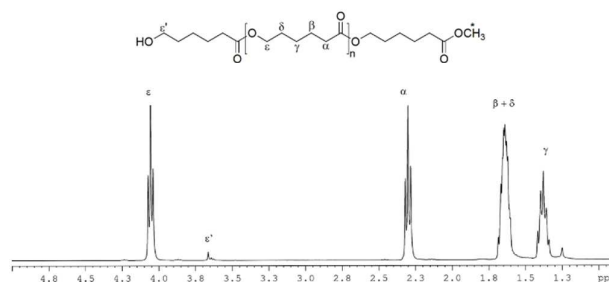


Figure 7. ¹H NMR spectrum (CDCl₃, 298 K) of polycaprolactone sample obtained using [ϵ -CL]/[MeOH]/[**1**] = 20/1/1 molar ratio.

With the aim to achieve a better control on the polymerization reaction, we tested the catalytic behavior of complex **1** in the presence of an alcohol. Indeed, in the presence of 1 or 2 equiv. of methanol, an improved productivity and a more efficient control of the molecular weights were achieved, as demonstrated by the better agreement between the theoretical and experimental values and by narrow molecular weight distributions (Table 2, runs 3 and 4 vs. 1). For complex **1**, the activity dropped down when the polymerization reaction was performed in CH₂Cl₂ (run 6, Table 2). This solvent effect has been some times observed for different metal initiators.^{38, 39}

The ¹H NMR analysis of a low molecular weight sample obtained by conversion of 20 equivalents of ϵ -CL by **1**/MeOH, revealed that the polymer chains were end-capped by one

Table 2. Polymerization of ϵ -CL initiated by complex **1** and **2**^a

Run	Cat	[ROH] (eq)	T (°C)	Time (min)	Conv. ^b (%)	Mn _{GPC} ^c (x 10 ³)	Mn _{theor} ^d (x 10 ³)	PDI ^c
1	1	0	25	100	72	119.1	16.4	1.09
2 ^e	1	0	100	5	100	130.5	22.8	1.69
3	1	1	25	60	94	34.7	21.6	1.06
4	1	2	25	60	100	21.1	11.4	1.10
5	1	2	50	15	86	26.1	9.8	1.04
6 ^e	1	1	25	60	35	21.2	8.0	1.05
7	2	0	25	100	0	-	-	-
8	2	1	25	60	0	-	-	-
9 ^f	2	1	100	720	100	11.4	22.8	1.37

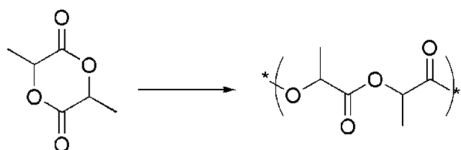
^aAll reactions were performed using 10 μ mol of either **1** or **2** in 2 mL of toluene, with 200 equiv. of ϵ -CL; ROH = MeOH. ^bConversion of ϵ -CL as determined by ¹H NMR spectral data. ^cExperimental M_n (in g/mol) and M_w/M_n (PDI) values determined by GPC in THF against polystyrene standards and using the corrected factor of 0.56. ^d Mn_{theor} (in g/mol) = 114.14 x ([ϵ -CL]₀/[MeOH]₀) x conversion ϵ -CL. ^e2 mL of methylene chloride. ^f2 mL of xylene, ROH = BnOH.

methyl ester -OCH₃ and a hydroxyl -CH₂CH₂OH (ϵ') group. This suggested that the initiation occurred through the insertion of the methoxide group into the monomer and the termination by hydrolysis of the growing chain (Figure 7).

The M_n values evaluated by NMR (8.7 Kg/mol) and the M_n values measured by GPC agreed perfectly, although they were higher than the theoretical value (2.3 Kg/mol).

Zinc complex **2** was tested as well for the ROP of ϵ -CL. It was found to be inactive at room temperature, even after the addition of one equivalent of methanol (run 7 vs 1 and 8 vs 3 in table 1). A moderate activity was observed only at high temperature (100 °C) and in the presence of one equivalent of alcohol (run 9 in table 2). The lower activity of the zinc catalyst in comparison to the homologous magnesium complex was in agreement with the lower ionic character of the Zn (2+) site than that of the Mg (2+) site.

Ring opening polymerization of lactide

**Scheme 3.** Ring opening polymerization of lactide.

Complexes **1** and **2** were also tested as initiators in the ROP of L-lactide and *rac*-lactide (Scheme 3). Representative results are summarized in Table 3. In the polymerization of L-lactide, **1**/BnOH system showed very high activity: at 50 °C, the quantitative conversion of 200 equivalents of monomer was achieved in less than 5 minutes (run 10, Table 3). The turn over frequency (TOF) was 2400 h⁻¹ and it can be annovered among the highest activities reported for lactide polymerization.⁴⁰ The high activity was preserved also performing the polymerization reactions at room temperature in methylene chloride (run 12). The reactivity of complex **1** toward L-lactide was higher than that toward ϵ -CL under comparable polymerization conditions (cf. run 10 of Table 3 vs. run 5 of Table 2 and run 12 of Table 3 vs. run 5 of Table 2). This behavior is uncommon, since polymerization of ϵ -CL is frequently faster than that of lactide, although some examples of zinc complexes with opposite reactivity towards these two monomers have been recently reported.¹⁰

A homonuclear decoupled ¹H NMR spectrum to determine the tacticity did not show any racemization within the polymer.

Catalyst **1** was found to exhibit the same activity when LA was used in its racemic form producing an atactic polymer.

As already observed in the ROP of ϵ -CL, complex **2** showed catalytic activity only at high temperature (100 °C) allowing the almost quantitative conversion of the monomer after 12 hours.

Table 3. Polymerization of L-LA initiated by complex **1** and **2**^a

Run ^a	Cat	Solvent	T (°C)	Time (min)	Conv. ^b (%)	M _{nGPC} ^c (10 ³)	M _{nth} ^d (10 ³)	PDI ^f
10	1	Tol	50	5	100	16.3	14.4	1.18
11	2	Tol	50	240	0	-	-	-
12	1	CH ₂ Cl ₂	25	10	97	12.1	13.1	1.20
13	2	Xylene	100	720	90	19.5	13.0	1.22

^aAll reactions were performed using 10 μmol of either **1** or **2** in 5 mL of solvent with [L-LA]₀/([I]₀/[ROH]) = 200: 1: 2. ^bConversion of L-LA as determined by ¹H NMR spectral data. ^cExperimental Mn (in Kg/mol) and M_w/M_n values determined by GPC in THF against polystyrene standards and using the corrected factor of 0.58. ^dM_ntheor (in g/mol) = 144.13 x ([L-LA]₀/[ROH]₀) x conversion L-LA.

Mechanistic investigations.

There are two main mechanisms for the ROP of the cyclic esters: the *coordination/insertion* mechanism, generally observed for metal initiators and the *activated monomer* mechanism, which is mostly promoted by organocatalysts.

According to the coordination/insertion mechanism, the initiation reaction involves coordination of the monomer at the Lewis acidic metal centre by its ketonic oxygen, resulting in activation of ligand X bounded to the metal (typically X = OH, OR, alkyl, or NR₂ group). This leads to ring-opening of the coordinated ligand and generation of a metal-alkoxide bond.

In the activated monomer mechanism, the cyclic ester is activated *via* the coordination to the metal centre and the initiation reaction occurs when the alcohol reacts with the activated monomer to form a ring-opened adduct. Such a mechanism has been previously proposed for a series of metal complexes.⁴⁰⁻⁴²

To establish which of the two mechanisms is operative, the polymerization reactions of ε-caprolactone promoted by complexes **1** and **2**, both in the absence and in the presence of alcohol, were monitored by ¹H NMR analysis. Initially the polymerization reaction of 20 equivalents of ε-caprolactone promoted by complex **1** was carried out at room temperature and in benzene-d₆ solution and was monitored by ¹H NMR analysis. As shown in the ¹H NMR spectra reported in Figure 8, when the monomer was added to the solution of complex **1**, most of the signals remained unchanged. No insertion of the monomer into the metal-pyrrolyl bonds of the homoleptic species was observed. The only significant variation was related to the two signals attributed to the methyls of the isopropyl groups that collapsed into a single broad peak. At the same time, additional resonances corresponding to the formation of PCL sequences were observed. These observations are consistent with the hypothesis that, in the presence of the monomer, the nitrogen atoms of the imine

fragments leave the metal centre allowing the coordination of caprolactone through the exocyclic oxygen atom of its carbonyl group. Subsequently, the monomer coordinated at the magnesium centre becomes susceptible to the attack by nucleophilic impurities (presumably traces of water) present in the polymerization medium. When the monomer was consumed, the mobile imine arms of the ancillary ligand coordinate again to the metal centre, as suggested by the signals of the methyls appearing again as two doublets.

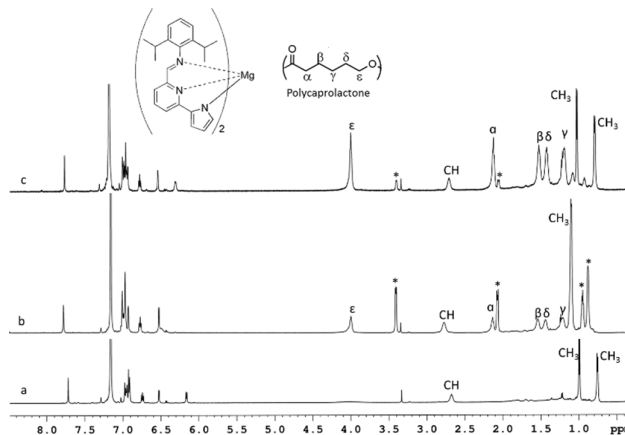
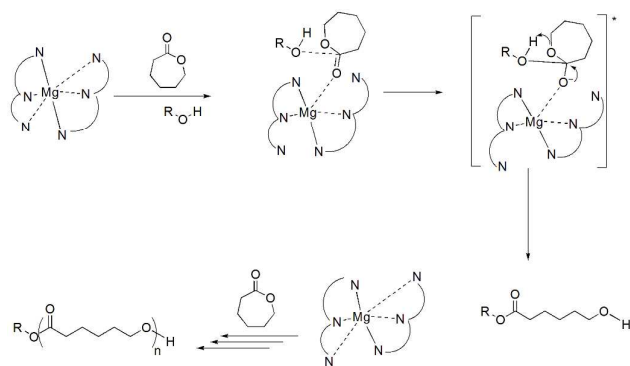


Figure 8. Monitoring of reaction of complex **1** with ε-caprolactone by ¹H NMR spectra (C₆D₆, RT, 400 MHz): a) Complex **1**; b) Complex **1** with ε-CL(*) at the beginning of reaction; c) The end of reaction when polymer was formed.

Thus, for complex **1**, an “activated-monomer” mechanism is suggested in which the coordinative flexibility of the ligand at the magnesium centre plays a role in catalytic activity (Scheme 4).

complex **2**. No reaction took place at room temperature even after prolonged reaction times, as observed in the polymerization runs: the NMR spectra showed exclusively the signals of the metal complex and of the unreacted monomer. Since the zinc complex showed catalytic activity only in the presence of alcohol, we monitored by NMR spectroscopy the reaction between complex **2** and 2 equivalents of benzyl alcohol in C_6D_6 . After 24 h at room temperature, the spectrum excluded any exchange between the ancillary ligand and the alcohol (i.e. the ligand was not displaced from the metal centre). Compound **2** revealed to be perfectly stable toward alcoholysis, even when the experiment was performed at high temperature (100 °C) and in the presence of an excess of BnOH, i.e. under conditions similar to or more drastic than those used in polymerizations.⁴³ The lack of reactivity of compound **2** toward alcoholysis suggested that, also in this case, the ring opening polymerization likely proceeds *via* an “activated monomer” mechanism.



Scheme 4. “Activated monomer” mechanism for ROP of ϵ -CL promoted by complex **1**.

This hypothesis was supported by *in situ* NMR monitoring the reaction of **2** with 20 equivalents of ϵ -CL in the presence of BnOH: after a few minutes, new resonances corresponding to the product of ring-opening insertion of BnOH into ϵ -CL (benzyl-6-hydroxyhexanoate), were observed while all resonances relative to the complex **2** remained unchanged (Figure S7 and S8). When all the monomer was consumed, the recorded 1H NMR spectra displayed the production of $BnO[C(=O)(CH_2)_5O]_n-H$ species (Figure S9).

On the basis of these findings combined with end-group analyses (ESI-MS 1H -NMR, Figures S9-S10) of the obtained polymers, we suggest that ROP mediated by **2**/BnOH proceeds via an “activated monomer” mechanism, as proposed for **1**.

Experimental

All manipulations of air- and/or water-sensitive compounds were carried out under a dry nitrogen atmosphere using an Mbraun Labmaster dry box or standard Schlenk-line techniques. Glassware and vials used in the polymerizations were dried in an oven at 120 °C overnight and exposed to vacuum–nitrogen cycles three times. All solvents were distilled over sodium benzophenone. $ZnEt_2$ and $Mg(n-Bu)_2$ (Aldrich) were used as received. CD_2Cl_2 , C_7D_8 and C_6D_6 were dried using molecular sieves. Lactide (Aldrich) was purified by crystallization from dry toluene. ϵ -CL (Aldrich) was dried with CaH_2 for 24 h at room temperature and then distilled under reduced pressure. All other chemicals were commercially available and used as received unless otherwise stated. All prolignands were prepared according to a published procedure.¹⁴

Instruments and measurements

The NMR spectra were recorded on a Bruker Advance 400 and a Bruker 600 MHz Ascend 3 HD spectrometers. Chemical shifts (δ) are expressed as parts per million. 1H NMR spectra are referenced using the residual solvent peak at δ 7.16 for C_6D_6 , δ 2.08 for C_7D_8 and δ 5.32 for CD_2Cl_2 . ^{13}C NMR spectra are referenced using the residual solvent peak at δ 128.06 for C_6D_6 , and δ 53.84 for CD_2Cl_2 . The molecular weights (M_n and M_w) and the molecular mass distribution (M_w/M_n) of polymer samples were measured by gel permeation chromatography (GPC) at 30 °C, using THF as solvent, an eluent flow rate of 1 mL/min, and narrow polystyrene standards as reference. The measurements were performed on a Waters 1525 binary system equipped with a Waters 2414 RI detector using four Styragel columns (range 1 000–1 000 000 Å). Mass spectrometry analyses were carried out using a Bruker Solarix XR Fourier transform ion cyclotron resonance mass spectrometer (Bruker Daltonik GmbH, Bremen, Germany) equipped with a 7 T refrigerated actively-shielded superconducting magnet (Bruker Biospin, Wissembourg, France). The samples were ionized in positive ion mode using the ESI ion source (Bruker Daltonik GmbH, Bremen, Germany). The mass range was set to m/z 150 – 3000. Mass calibration: The mass spectra were calibrated externally using a NaTFA solution in positive ion mode. A linear calibration was applied.

Synthesis of complexes

Synthesis of complex 1. In an Mbraun glovebox, a solution of the prolignand (0.200 g, 0.603 mmol) in benzene (2 mL) was added dropwise into a stirred benzene solution of $MgBu_2$ (603 μ L of a 1.0 M solution in heptane, 0.603 mmol). The resulting mixture was stirred at room temperature for 2 hours. The solvent was removed in vacuo and the solid residue was washed using dry pentane to obtain 0.400 g of deep orange solid (yield = 96%). Suitable crystals for X-ray analysis were obtained dissolving the magnesium complex in toluene, at -20 °C. ESI(+)–MS analysis: calcd for $C_{44}H_{48}MgN_6$ m/z 684.37, found (ion) m/z : $[MH^+]$ 685.39.

^1H NMR (CD_2Cl_2 , 298 K, 600 MHz, J values in Hz) δ 0.53 (d, 12H, $^3J_{\text{HH}} = 6.4$, $\text{CH}(\text{CH}_3)_2$), 0.91 (d, 12H, $^3J_{\text{HH}} = 6.4$, $\text{CH}(\text{CH}_3)_2$), 2.59 (sept, 4H, $^3J_{\text{HH}} = 6.4$, $\text{CH}(\text{CH}_3)_2$), 6.02 (dd, 2H, $^4J_{\text{HH}} = 1.6$, $^3J_{\text{HH}} = 3.0$, H2), 6.42 (t, 2H, $^4J_{\text{HH}} = 1.0$, $^3J_{\text{HH}} = 1.6$, H1), 6.72 (dd, 2H, $^4J_{\text{HH}} = 1.0$, $^3J_{\text{HH}} = 3.0$, H3), 6.93 (d, 4H, $^3J_{\text{HH}} = 8.0$, H13, H15), 7.01 (t, 2H, $^3J_{\text{HH}} = 8.0$, H14), 7.05 (dd, 2H, $^4J_{\text{HH}} = 1.0$, $^3J_{\text{HH}} = 7.0$, H8), 7.50 (dd, 2H, $^4J_{\text{HH}} = 1.0$, $^3J_{\text{HH}} = 8.5$, H6), 7.65 (dd, 2H, $^4J_{\text{HH}} = 7.0$, $^3J_{\text{HH}} = 8.5$, H7), 8.08 (s, 2H, H10).

^1H NMR (C_6D_6 , 298 K, 600 MHz, J values in Hz) δ 0.75 (d, 12H, $^3J_{\text{HH}} = 6.4$, $\text{CH}(\text{CH}_3)_2$), 0.99 (d, 12H, $^3J_{\text{HH}} = 6.4$, $\text{CH}(\text{CH}_3)_2$), 2.67 (sept, 4H, $^3J_{\text{HH}} = 6.4$, $\text{CH}(\text{CH}_3)_2$), 6.16 (dd, 2H, $^4J_{\text{HH}} = 1.0$, $^3J_{\text{HH}} = 7.0$, H8), 6.52 (dd, 2H, $^4J_{\text{HH}} = 1.6$, $^3J_{\text{HH}} = 3.0$, H2), 6.74 (dd, 2H, $^4J_{\text{HH}} = 7.0$, $^3J_{\text{HH}} = 8.5$, H7), 6.91 (dd, 2H, $^4J_{\text{HH}} = 1.0$, $^3J_{\text{HH}} = 3.0$, H3), 6.93 (b, 4H, H13, H15), 6.95 (b, 2H, H14), 6.95 (dd, 2H, $^4J_{\text{HH}} = 1.0$, $^3J_{\text{HH}} = 8.5$, H6), 6.98 (dd, 2H, $^4J_{\text{HH}} = 1.0$, $^3J_{\text{HH}} = 1.6$, H1), 7.72 (s, 2H, H10).

^{13}C NMR (C_6D_6 , 298 K, 151 MHz) δ 25.05 (8C, $\text{CH}(\text{CH}_3)_2$), 28.71 (4C, $\text{CH}(\text{CH}_3)_2$), 113.09 (C2), 113.12 (C3), 119.21 (C8), 122.15 (C6), 123.62, (C13, C15), 126.42 (C14), 129.16 (C12, C16), 136.03 (C1), 136.77 (Cq), 138.54 (C7), 147.32 (Cq), 147.88 (Cq), 157.09 (Cq) 164.79 (C10).

Synthesis of complex 2. In an Mbraun glovebox, a benzene solution of the proligand (0.200 g, 0.603 mmol) (2 mL) was slowly added to a solution of ZnEt_2 (0.075 g, 0.604 mmol) or of $\text{Zn}[\text{N}(\text{SiMe}_3)_2]_2$ (0.233 g, 0.604 mmol) in the same volume of benzene at room temperature. The resulting solution was stirred at the same temperature for 2 hours, and then the solvent was removed in vacuo. The solid residue was washed twice using dry pentane and dried under vacuum for several hours to give 0.430 g of red compound (yield = 98%). ESI(+) - MS analysis: calcd for $\text{C}_{44}\text{H}_{48}\text{N}_6\text{Zn}$ m/z 724.32, found (ion) m/z: $[\text{MH}^+]$ 725.35.

^1H NMR (CD_2Cl_2 , 298 K, 600 MHz, J values in Hz) δ 0.80 (d, 12H, $^3J_{\text{HH}} = 6.8$, $\text{CH}(\text{CH}_3)_2$), 0.91 (d, 12H, $^3J_{\text{HH}} = 6.8$, $\text{CH}(\text{CH}_3)_2$), 2.36 (sept, 4H, $^3J_{\text{HH}} = 6.8$, $\text{CH}(\text{CH}_3)_2$), 6.18 (dd, 2H, $^4J_{\text{HH}} = 1.6$, $^3J_{\text{HH}} = 3.0$, H2), 6.73 (dd, 2H, $^4J_{\text{HH}} = 1.0$, $^3J_{\text{HH}} = 1.6$, H3), 6.80 (d, 2H, $^3J_{\text{HH}} = 1.0$, H1), 6.95 – 7.01 (m, 6H, H13, H14), 7.45 (d, 2H, $^3J_{\text{HH}} = 8.0$, H8), 7.50 (d, 2H, $^3J_{\text{HH}} = 8.0$, H6), 7.66 (t, 2H, $^3J_{\text{HH}} = 8.0$, H7), 7.82 (s, 2H, H10).

^{13}C NMR (CD_2Cl_2 , 298 K, 151 MHz) δ 23.80 (8C, $\text{CH}(\text{CH}_3)_2$), 27.98 (4C, $\text{CH}(\text{CH}_3)_2$), 111.12 (C3), 113.09 (C2), 119.17 (C8), 121.19 (C6), 122.91, (C13), 124.82 (C14), 132.88 (C1), 135.07 (C11), 137.50 (C12), 139.81 (C7), 148.12 (C5), 149.17 (C4), 155.04 (C9) 160.26 (C10).

X-ray crystallography

Crystals of **1** and **2** were selected and mounted on a cryoloop with paratone oil and measured at 100 K. Single crystal diffraction experiments were performed by means of a Rigaku AFC7S diffractometer equipped with a Mercury² CCD detector

using graphite monochromated MoK α radiation ($\lambda = 0.71069$ Å). Data reduction was performed with the crystallographic package CrystalClear.⁴⁴ Data were corrected for Lorentz, polarization and absorption. For compound **1** the structure was achieved by VLD procedure as implemented in the program SIR2011⁴⁵ and refined by means of full matrix least-squares based on F^2 using the program SHELXL2014.⁴⁴ There are also two crystallographically independent toluene molecules, one being located around an inversion centre. To model the positional disorder two toluene molecules with opposite orientation were considered and refined as a rigid group with isotropic displacement parameters. With the exception of the disordered toluene molecule, non-hydrogen were refined anisotropically, hydrogen atoms were positioned geometrically and included in structure factors calculations and refined with riding coordinates. For compound **2** indexing suggested either an orthogonal unit cell ($a=19.997(5)$ Å, $b=21.592(5)$ Å, $c=21.6157(5)$ Å) or a tetragonal unit cell ($a=21.571(3)$ Å, $c=19.990(3)$ Å). Several possible space groups were considered in the attempt to solve the structure by direct methods or by using the VLD procedure,⁴⁵ but no satisfactory structure model was found. Thus, crystals of **2** were inserted in a Lindeman capillary under inert atmosphere and measured at 293 K. The collected data were indexed considering a monoclinic unit cell ($a=20.124(3)$ Å, $b=19.606(3)$ Å, $c=21.718(3)$ Å, $\beta=94.445(4)^\circ$). The structure was solved by VLD procedure²² and refined by means of full matrix least-squares based on F^2 using the program SHELXL2014.⁴⁶ A toluene molecule is located on a two-fold axis, thus there is half molecule of toluene per each zinc complex. Non-hydrogen were refined anisotropically, hydrogen atoms were positioned geometrically and included in structure factors calculations and refined with riding coordinates. Idealized methyl hydrogen atoms were refined as a rotating group. Crystal data and refinement details are reported in Table 4. Crystal structures were drawn using OLEX2.⁴⁷ It is to note that further attempts to solve the data collected at 100 K for compound **2** considering a monoclinic unit cell were also unsuccessful.

Polymerization of lactide and ϵ -caprolactone

In a typical polymerization, a magnetically stirred reactor vessel was charged with a solution of metal initiator ($[\text{M}] = 1.5$ M) in the appropriate solvent, to which the alcohol was eventually added, and then a prescribed amount of monomer. The reaction mixture was immediately stirred with a magnetic stir bar at predicted temperature for the prescribed time. After specified time an aliquot of the crude material was sampled and quenched in wet CDCl_3 . The sample was subjected to monomer conversion determination, which was monitored by integration of monomer versus polymer in ^1H -NMR spectrum. The reaction mixture was dissolved, therefore quenched, in CHCl_3 and precipitated in methanol. The obtained polymer was collected by filtration and further dried in a vacuum oven at 60°C for 16 h.

Table 4. Crystal data and refinement details for compounds **1** and **2**.

	1	2
Temperature (K)	100	293
Moiety formula	2 C ₄₄ H ₄₈ N ₆ Mg 3·C ₇ H ₈	2·C ₄₄ H ₄₈ N ₆ Zn·C ₇ H ₈
Formula weight	1646.79	1544.68
Crystal system	Monoclinic	Monoclinic
Space group	<i>P</i> 2 ₁ / <i>c</i>	<i>C</i> 2/ <i>c</i>
<i>a</i> (Å)	18.885(4)	20.124(3)
<i>b</i> (Å)	12.5765(19)	19.606(3)
<i>c</i> (Å)	21.644(4)	21.718(3)
β (°)	115.462(4)	94.445(4)
<i>V</i> (Å ³)	4641.3(14)	8543(2)
<i>Z</i>	2	4
<i>Z'</i>	0.5	0.5
<i>D</i> _c (g/cm ³)	1.178	1.201
<i>F</i> (000)	1764	3272
Wavelength (Å)	0.7107	0.7107
absorption coeff (mm ⁻¹)	0.082	0.601
absorption correction	multi-scan	multi-scan
transmission factors	0.973, 0.988	0.613, 1.000
n. of var.	546	482
<i>R</i> 1 (<i>I</i> > 2 σ (<i>I</i>))	0.0864 (5486)	0.0968 (3939)
<i>wR</i> 2 (all data)	0.2189 (11395)	0.3286 (9114)
goodness of fit	1.010	0.999
max and min diff.	0.60, -0.32	0.57, -1.00
Fourier (e/Å ³)		

Conclusions

Homoleptic magnesium and zinc complexes derived from a pyrrolylpyridylimino proligand were synthesized and characterized. X-ray diffraction studies demonstrated that the magnesium complex has an octahedral geometry in which the two tridentate ligands are coordinated around the metal in an approximately perpendicular arrangement. Differently, in the analogous zinc complex the ligands act as bidentate ligands and a four-coordinate metal centre resulted in the solid state. Detailed NMR studies showed that these complexes preserve the same coordination also in solution.

The magnesium complex **1**, in the presence of an exogenous alcohol, efficiently promotes the polymerization of ϵ -caprolactone and lactide under mild reaction conditions. For the zinc complex **2**, moderate activities were observed when the reactions were performed at high temperature (100°C), in line with literature results for related zinc initiators.

NMR studies of the polymerization reactions, in combination with chain end analysis of the obtained polymers, demonstrated that, for both complexes, activated monomer mechanisms are operative. At least in the case of the magnesium complex, the mechanism is assisted by the coordinative flexibility of the ancillary ligands, as demonstrated by *in situ* NMR studies.

These findings confirm that homoleptic complexes of divalent

performing initiators operating *via* an “activated monomer” mechanism.

Conflict of interest

There are no conflicts to declare.

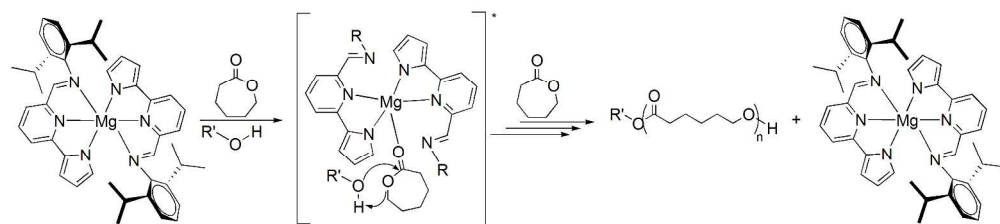
Acknowledgements

This work was financially supported by the University of Salerno (Fondo di Ateneo Ricerca di Base). I. D’A. acknowledges a fellowship granted by the Italian Consortium Chemical Reactivity and Catalysis, CIRCC (Progetto competitivo MIUR). The authors thank Dr. Patrizia Oliva for IR assistance and Dr. Patrizia Iannece for Mass spectrometry analyses.

Notes and references

- S. Mecking, *Angew. Chem., Int. Ed.*, 2004, **43**, 1078-1085.
- A.-C. Albertsson and I. K. Varma, *Biomacromolecules*, 2003, **4**, 1466-1486.
- R. H. Platel, L. M. Hodgson and C. K. Williams, *Polymer Reviews*, 2008, **48**, 11-63.
- P. J. Dijkstra, H. Du and J. Feijen, *Polym. Chem.*, 2011, **2**, 520-527.
- C. A. Wheaton, P. G. Hayes and B. J. Ireland, *Dalton Trans.*, 2009, 4832-4846.
- S. Bellemin-Laponnaz and S. Dagorne, *Chem. Rev.*, 2014, **114**, 8747-8774.
- M. Bouyhay, Y. Sarazin, O. L. Casagrande and J.-F. Carpentier, *Appl. Organomet. Chem.*, 2012, **26**, 681-688.
- M. Lamberti, A. Botta and M. Mazzeo, *Appl. Organomet. Chem.*, 2014, **28**, 140-145.
- C. Gallegos, V. Taberner, F. M. García-Valle, M. E. G. Mosquera, T. Cuenca and J. Cano, *Organometallics*, 2013, **32**, 6624-6627.
- I. D’Auria, M. Lamberti, M. Mazzeo, S. Milione, G. Roviello and C. Pellicchia, *Chem. - Eur. J.*, 2012, **18**, 2349-2360.
- M. Huang and H. Ma, *Eur. J. Inorg. Chem.*, 2016, **2016**, 3791-3803.
- M. Cheng, A. B. Attygalle, E. B. Lobkovsky and G. W. Coates, *J. Am. Chem. Soc.*, 1999, **121**, 11583-11584.
- B. M. Chamberlain, M. Cheng, D. R. Moore, T. M. Ovitt, E. B. Lobkovsky and G. W. Coates, *J. Am. Chem. Soc.*, 2001, **123**, 3229-3238.
- M. H. Chisholm, J. Gallucci and K. Phomphrai, *Inorg. Chem.*, 2002, **41**, 2785-2794.
- M. Keram and H. Ma, *Appl. Organomet. Chem.*, DOI: 10.1002/aoc.3893, n/a-n/a.
- M. H. Chisholm, N. W. Eilerts, J. C. Huffman, S. S. Iyer, M. Pacold and K. Phomphrai, *J. Am. Chem. Soc.*, 2000, **122**, 11845-11854.
- C. Fliedel, S. Mameri, S. Dagorne and T. Aviles, *Appl. Organomet. Chem.*, 2014, **28**, 504-511.
- C. Fliedel, D. Vila-Vicosa, M. J. Calhorda, S. Dagorne and T. Aviles, *ChemCatChem*, 2014, **6**, 1357-1367.
- A. Pilone, M. Lamberti, M. Mazzeo, S. Milione and C.

20. C. K. Williams, L. E. Breyfogle, S. K. Choi, W. Nam, V. G. Young, Jr., M. A. Hillmyer and W. B. Tolman, *J. Am. Chem. Soc.*, 2003, **125**, 11350-11359.
21. L. Wang and H. Ma, *Macromolecules*, 2010, **43**, 6535-6537.
22. V. Poirier, T. Roisnel, J.-F. Carpentier and Y. Sarazin, *Dalton Trans.*, 2009, 9820-9827.
23. C. Fliedel, V. Rosa, F. M. Alves, A. M. Martins, T. Aviles and S. Dagorne, *Dalton Trans.*, 2015, **44**, 12376-12387.
24. M. Huang, C. Pan and H. Ma, *Dalton Trans.*, 2015, 12420-12431.
25. M. H. Chisholm, J. C. Gallucci, H. Zhen and J. C. Huffn, *Inorg. Chem.*, 2001, **40**, 5051-5054.
26. T. Rosen, I. Goldberg, W. Navarra, V. Venditto and M. Kol, *Chem. Sci.*, 2017, DOI: 10.1039/c7sc01514c, Ahead of Print.
27. T. Rosen, Y. Popowski, I. Goldberg and M. Kol, *Chem. - Eur. J.*, 2016, **22**, 11533-11536.
28. J. Ejfler, S. Szafert, K. Mierzwicki, L. B. Jerzykiewicz and P. Sobota, *Dalton Trans.*, 2008, 6556-6562.
29. J. Wojtaszak, K. Mierzwicki, S. Szafert, N. Gulia and J. Ejfler, *Dalton Trans.*, 2014, **43**, 2424-2436.
30. G. Li, M. Lamberti, M. Mazzeo, D. Pappalardo, G. Roviello and C. Pellecchia, *Organometallics*, 2012, **31**, 1180-1188.
31. G. Li, M. Lamberti, G. Roviello and C. Pellecchia, *Organometallics*, 2012, **31**, 6772-6778.
32. G. Li, C. Zuccaccia, C. Tedesco, I. D'Auria, A. Macchioni and C. Pellecchia, *Chem. Eur. J.*, 2014, **20**, 232-244. .
33. G. Li, M. Lamberti, S. D'Amora and C. Pellecchia, *Macromolecules*, 2010, **43**, 8887-8891.
34. L. Annunziata, D. Pappalardo, C. Tedesco and C. Pellecchia, *Organometallics*, 2009, **28**, 688-697.
35. K. A. Frazier, R. D. Froese, Y. He, J. Klosin, C. N. Theriault, P. C. Vosejka, Z. Zhou and K. A. Abboud, *Organometallics*, 2011, **30**, 3318-3329.
36. L. Annunziata, D. Pappalardo, C. Tedesco and C. Pellecchia, *Macromolecules*, 2009, **42**, 5572-5578.
37. The ligand mean plane is defined for each ligand by considering 14 nitrogen and carbon atoms, excluding the isopropyl substituted aromatic groups.
38. H. Ma, T. P. Spaniol and J. Okuda, *Inorg. Chem.*, 2008, **47**, 3328-3339.
39. K. Nie, L. Fang, Y. Yao, Y. Zhang, Q. Shen and Y. Wang, *Inorg. Chem.*, 2012, **51**, 11133-11143.
40. T. Rosen, I. Goldberg, V. Venditto and M. Kol, *J. Am. Chem. Soc.*, 2016, **138**, 12041-12044.
41. C. Bakewell, A. J. P. White, N. J. Long and C. K. Williams, *Inorg. Chem.*, 2013, **52**, 12561-12567.
42. Y. Sun, Y. Cui, J. Xiong, Z. Dai, N. Tang and J. Wu, *Dalton Trans.*, 2015, **44**, 16383-16391.
43. The same experiment performed with complex 1 indicate that the alcoholysis reaction is instantaneous on the laboratory timescale and results in the reduction of the ligand framework coordinated to the metal center.
44. CrystalClear, Crystal Structure Analysis Package, Rigaku-Molecular Structure Corp.
45. M. C. Burla, R. Caliandro, B. Carrozzini, G. L. Cascarano, C. Cuocci, C. Giacovazzo, M. Mallamo, A. Mazzone and G. Polidori, *J. Appl. Cryst.*, 2015, **48**, 306-309.
46. G. M. Sheldrick, *Acta Cryst.*, 2015, **C71**, 3-8.
47. O. V. Dolomanov, L. J. Bourhis, R. J. Gildea, J. A. K. Howard and H. Puschmann, *J. Appl. Cryst.*, 2009, **42**, 339-341



292x65mm (300 x 300 DPI)

Supporting Information

New homoleptic bis(pyrrolylpyridylimino) Mg(II) and Zn(II) complexes as catalysts for the ring opening polymerization of cyclic esters via an "activated monomer" mechanism.

Table of contents

Figure S1. ^1H NMR of complex 1 in C_6D_6	S2
Figure S2. ^{13}C NMR of complex 1 in C_6D_6	S2
Figure S3. ^1H ^{13}C HMQC spectrum of complex 1 in C_6D_6	S3
Figure S4. ^1H NMR of complex 2 in CD_2Cl_2	S4
Figure S5. ^{13}C NMR of complex 2 in CD_2Cl_2	S4
Figure S6. Sections of the ^1H COSY NMR and ^1H ^1H NOESY NMR of complex 2 in CD_2Cl_2	S5
Figure S7. ^1H NMR of a 20:10:1 mixture of BnOH, ϵ -CL and complex 2 in C_6D_6 , leading the formation of polycaprolactone.....	S6
Figure S8. An enlargement of ^1H NMR of a 20:10:1 mixture of BnOH, ϵ -CL and complex 2 in C_6D_6 , at first time of reaction.....	S7
Figure S9. ^1H NMR of a PCL sample obtained from the mixture of BnOH, ϵ -CL and complex 2 in C_6D_6	S7
Figure S10. MALDI-TOF mass spectrum of the mixture of complex 2 , BnOH and polycaprolactone.....	S8

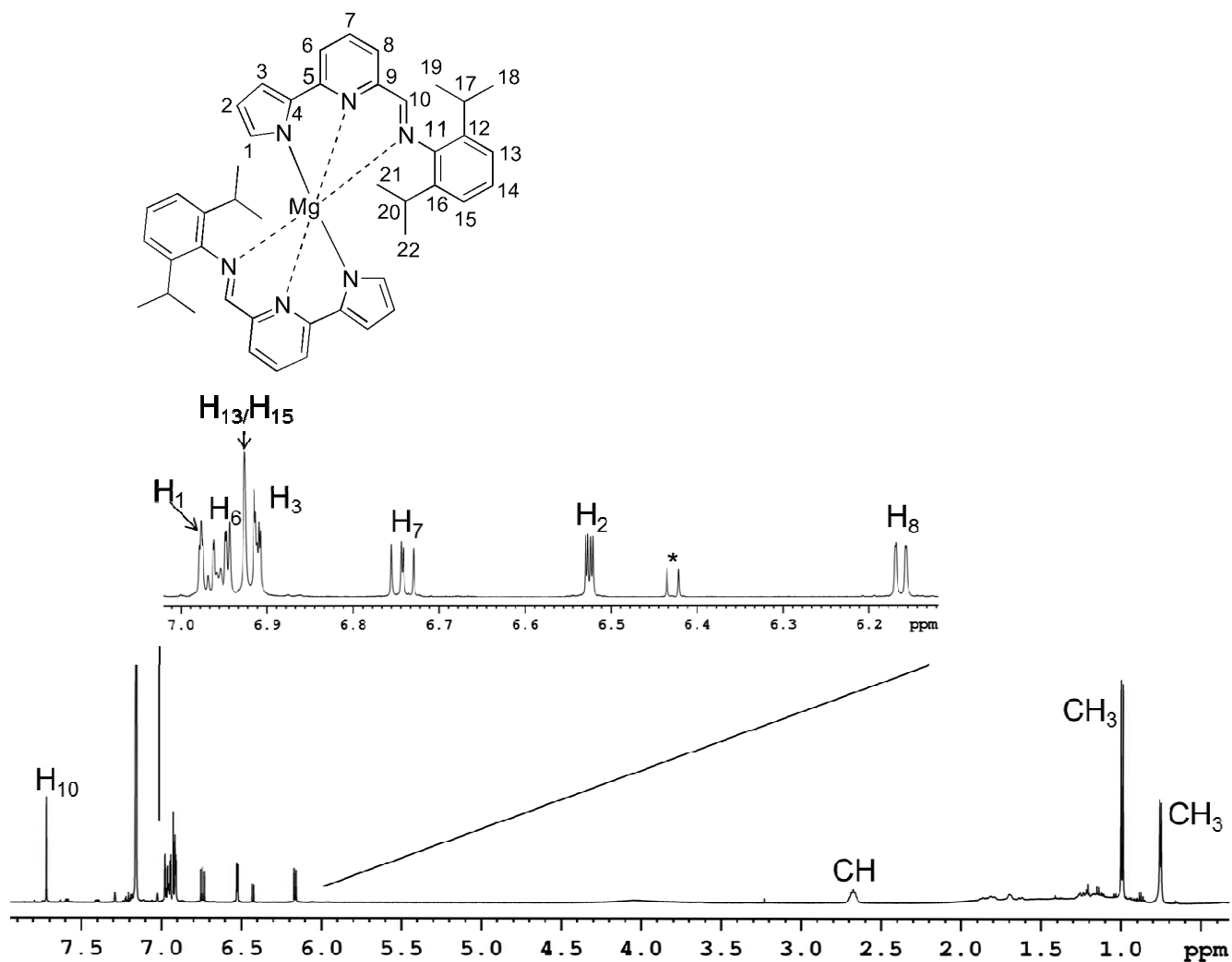


Figure S1. ^1H NMR spectrum (C_6D_6 , 298 K, 600 MHz) of complex 1.

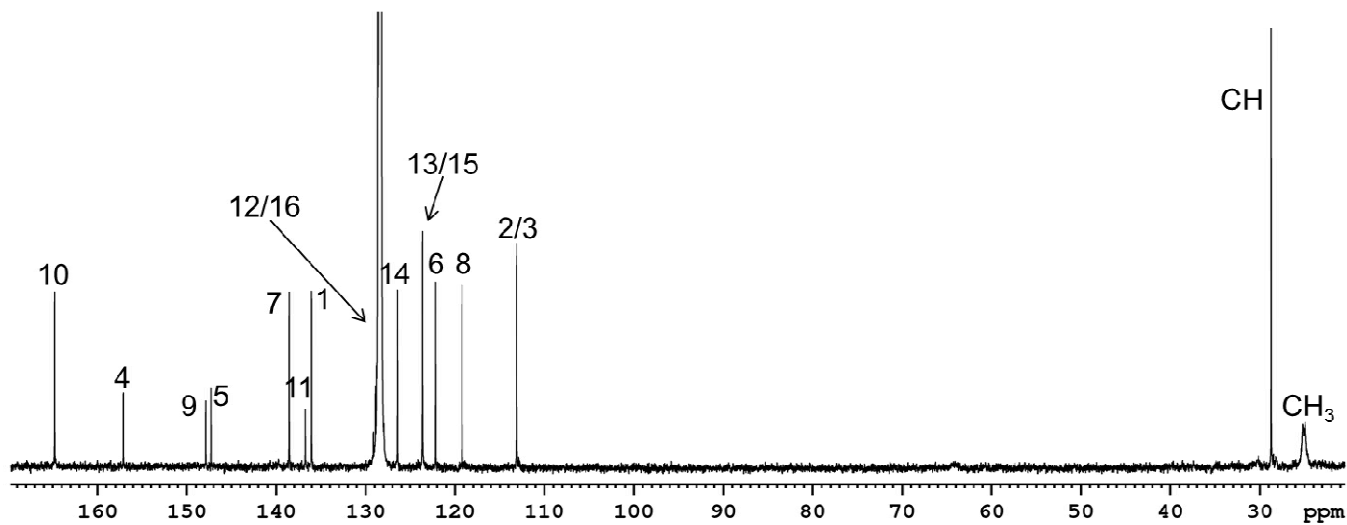


Figure S2. ^{13}C NMR spectrum (C_6D_6 , 298 K, 600 MHz) of complex 1.

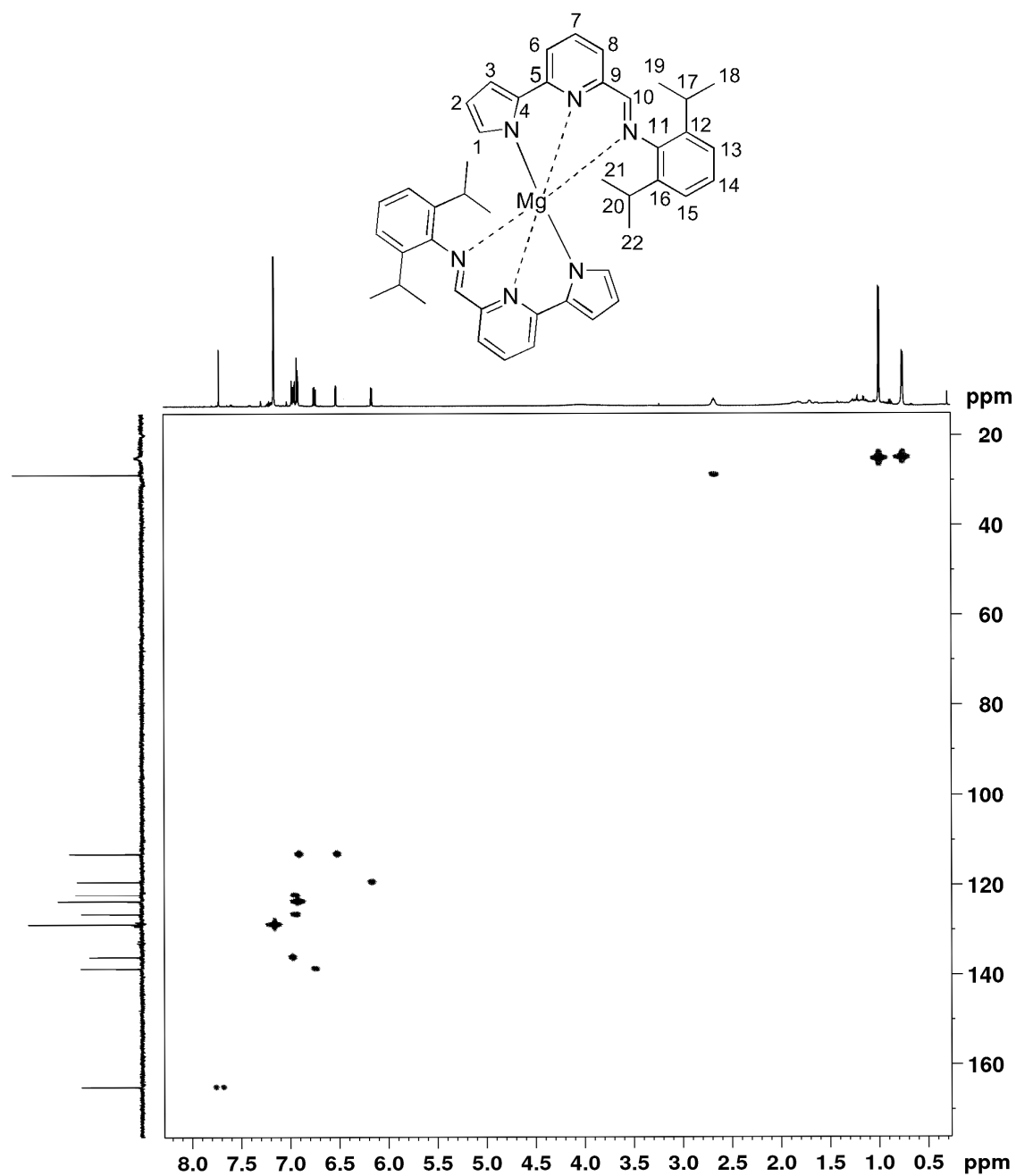


Figure S3. $^1\text{H } ^{13}\text{C}\{^1\text{H}\}$ HMQC spectrum (C_6D_6 , 298 K, 600 MHz) of complex 1

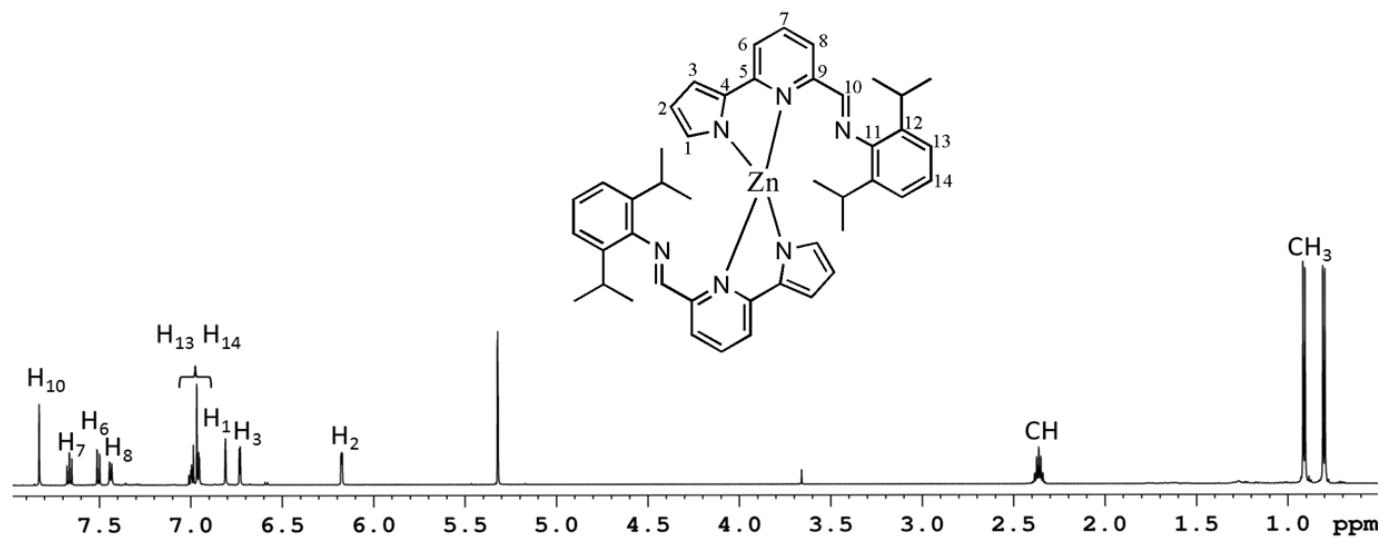


Figure S4. ¹H NMR spectrum (CD₂Cl₂, 298 k, 600 MHz) of complex 2.

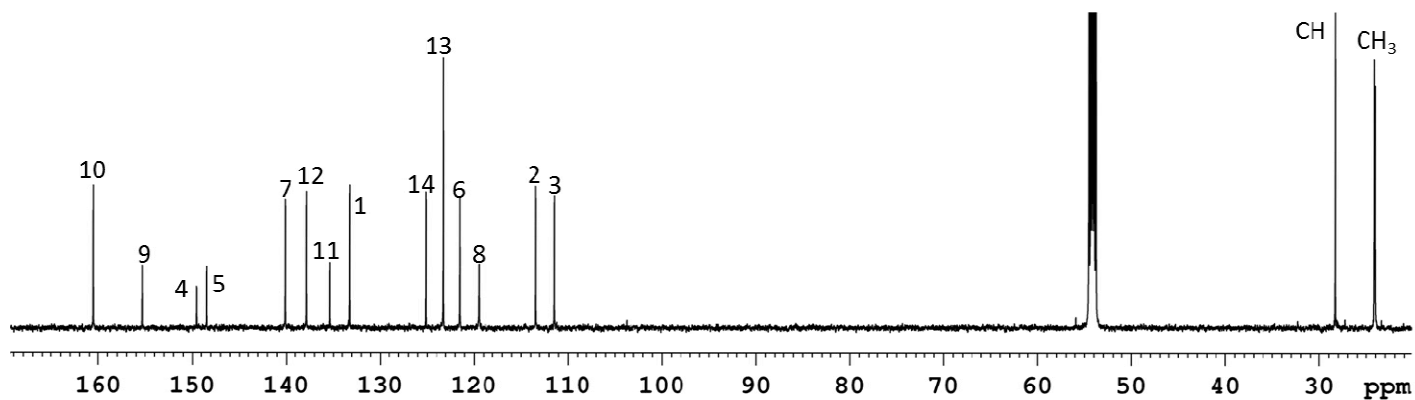


Figure S5. ¹³C NMR spectrum (CD₂Cl₂, 298 k, 600 MHz) of complex 2

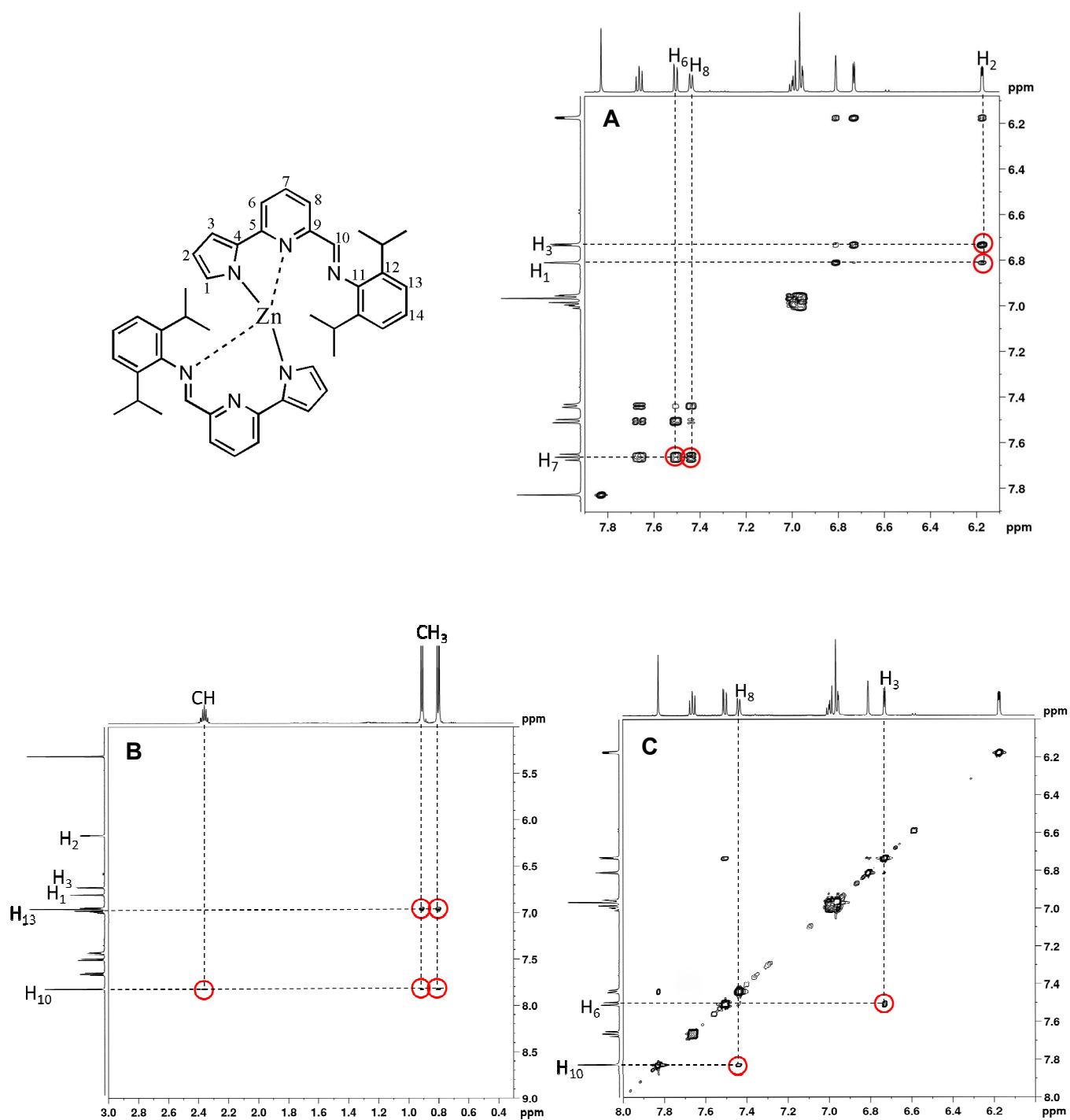


Figure S6. A: One section of the ¹H COSY NMR spectrum of **2** (CD₂Cl₂, 298 K, 600 MHz); B and C: two sections of ¹H ¹H NOESY NMR spectrum of **2** (CD₂Cl₂, 298 K, 600 MHz).

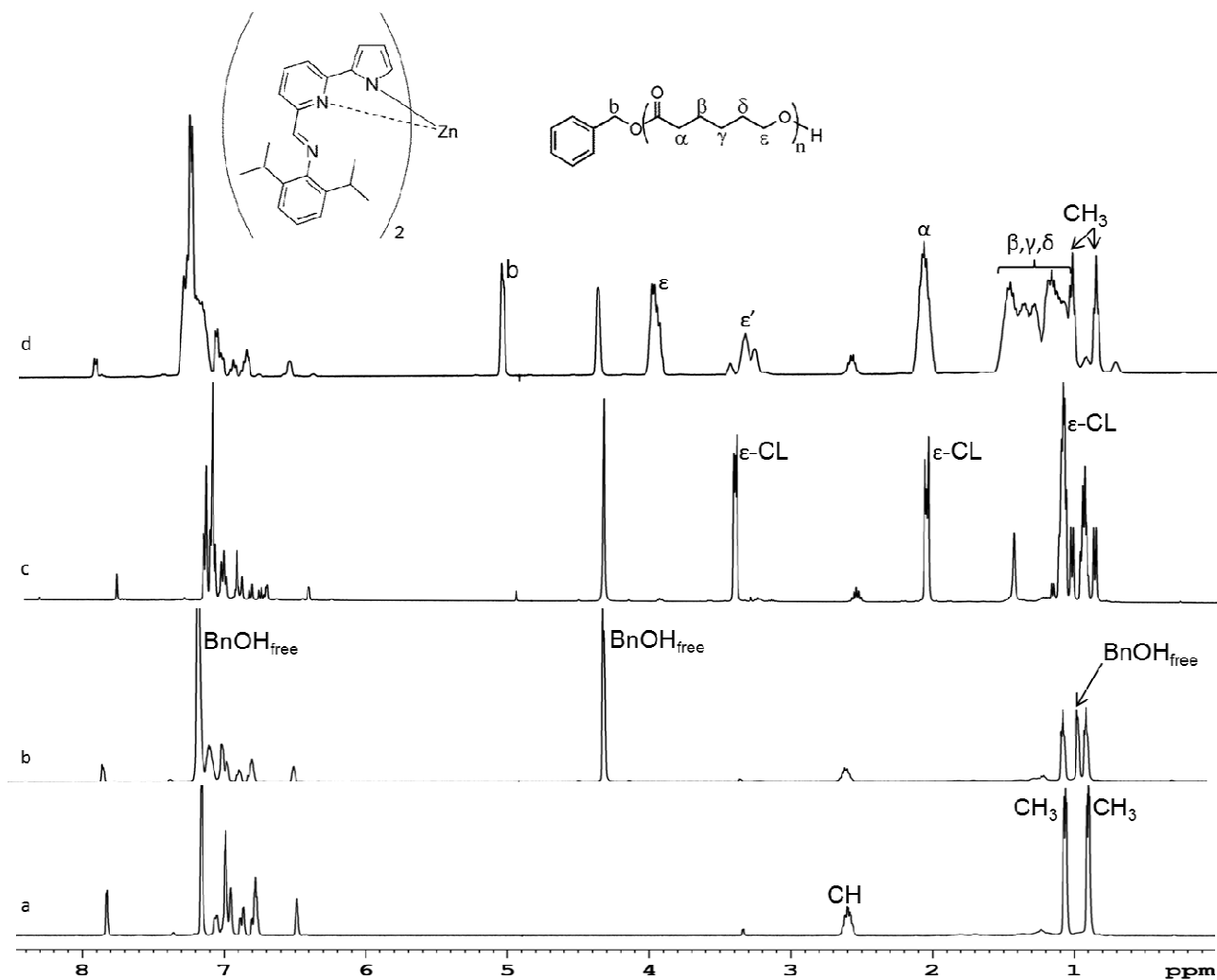


Figure S7. Monitoring of reaction by ^1H NMR spectra (C_6D_6 , 373K, 400 MHz) : a) Complex 2; b) Complex 2 with BnOH; c) Complex with BnOH and $\epsilon\text{-CL}$ at first time and d) Complex 2 with BnOH and oylcaprolactone at end of reaction.

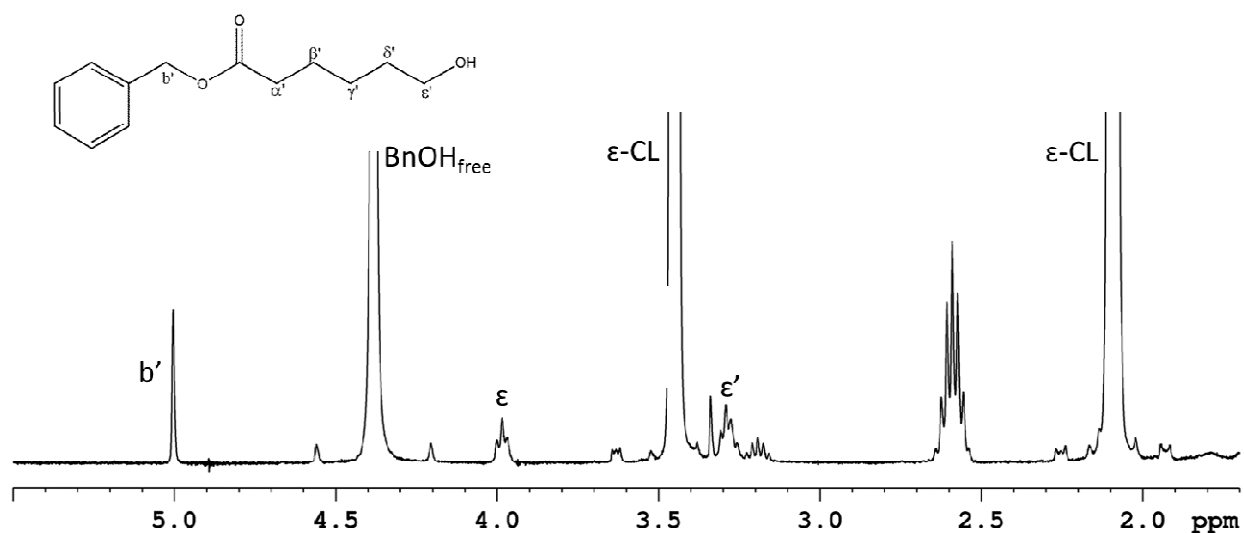


Figure S8. An enlargement of ^1H NMR spectrum *c* (figure 4) (C_6D_6 , 373K, 400 MHz) in which signals of benzyl-6-hydroxyhexanoate are showed.

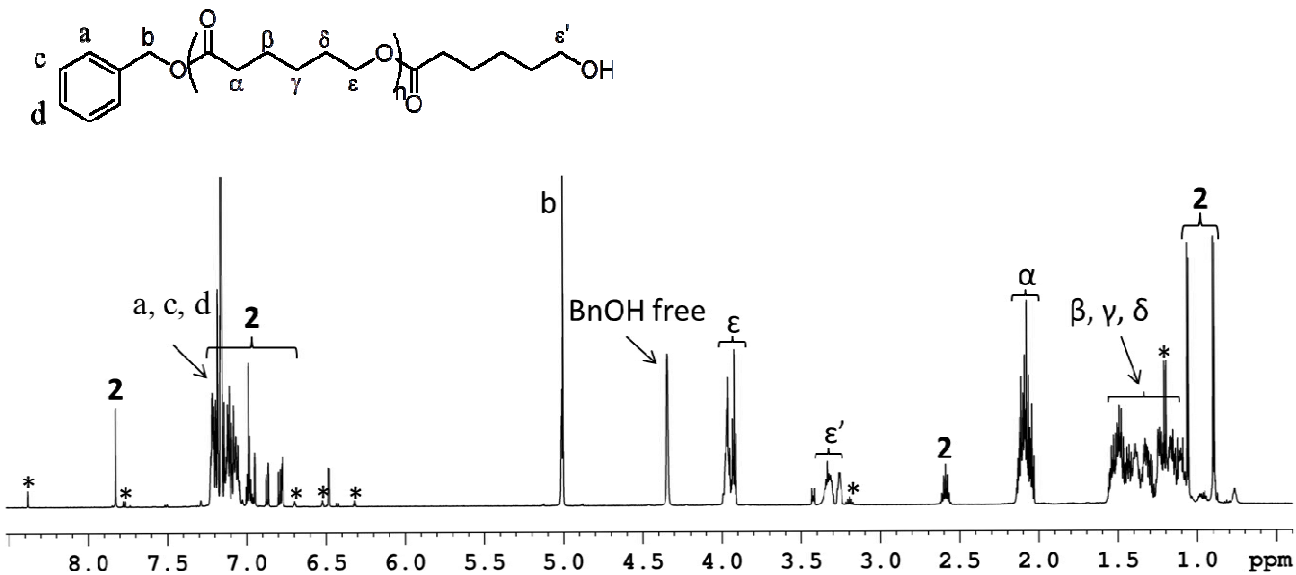


Figure S9. ^1H NMR spectrum (C_6D_6 , 298K, 400 MHz) of the mixture of complex **2**, BnOH and polycaprolactone at the end of reaction; signals with $*$ belong to traces of ligand.

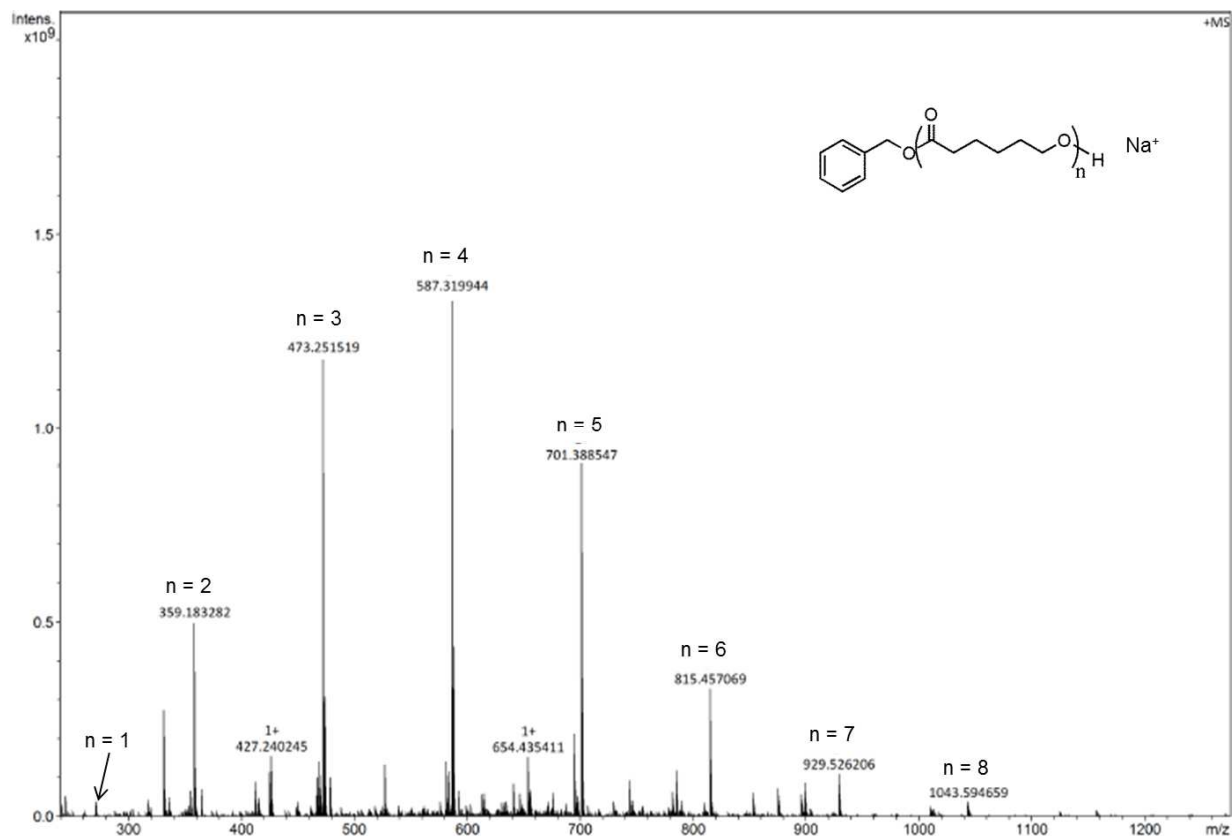


Figure S10. MALDI-TOF mass spectrum of the mixture of complex 2, BnOH and polycaprolactone.